π-Cation Radicals of Iron(III) Derivatives of Deformed Porphyrins†

Mangalampalli Ravikanth, Ashutosh Misra, Damodar Reddy and Tavarekere K. Chandrashekar*
Department of Chemistry, Indian Institute of Technology, Kanpur 208016, India

π-Cation radicals of iron(III) derivatives of some deformed porphyrins have been characterised using UV/VIS, IR and ^{1}H NMR spectroscopy and by magnetic susceptibility measurements. The deformation in these systems has been induced by a covalent attachment of short bridging chains across the porphyrin periphery. Molecular mechanics simulation clearly reveals the enforced deformation in the porphyrin cores of the free bases inferred from the multiplet structure for the pyrrole protons by ^{1}H NMR spectroscopy. Significant red shifts in Soret (171–340 cm^{-1}) and Q-band (76–354 cm^{-1}) absorption maxima for the iron(III) derivatives relative to [Fe(tpp)Cl] (H_2tpp = 5,10,15,20-tetraphenylporphyrin) implies the retention of deformation in solution. Collective evidence from IR, UV/VIS and ^{1}H NMR spectroscopy and magnetic susceptibility measurements suggests for the oxidised derivatives a high-spin iron(III) state ($S = \frac{5}{2}$) antiferromagnetically coupled to a porphyrin radical cation ($S = \frac{1}{2}$). Magnetic moment values (4.8–5.1 μ_B) measured for solids and CD_2Cl_2 solutions indicate an intramolecular d–π coupling facilitated through an antiferromagnetic exchange. These results substantiate the emerging correlation between the structure of the macrocycle and the metal–ligand magnetic interactions in high-spin iron(III) porphyrin radical-cation complexes.

The involvement of metalloporphyrin π-cation radicals as intermediates in biological systems containing haem proteins such as peroxidases and catalases is well documented in the literature.[1–4] The interaction between the unpaired electrons in iron and the porphyrin ring affects the electronic structure of the metalloporphyrin thereby altering the magnetic properties. For example, the magnetic coupling between the porphyrin π-cation radical and the iron(IV)–oxo unit in Horseradish peroxidase-I (HRP-I) is shown to be weakly antiferromagnetic ($J \leqslant 0.1\ D$, where D is zero-field splitting parameter)[1] while it is strongly antiferromagnetic ($J = 1.02D$) in chloroperoxidase-I (CPO-I).[4] Model compound studies to date on metallo-octaethylporphyrins and metallotetraphenylporphyrins have established that the spin coupling mechanism between the metal centre and the porphyrin ring is highly sensitive to the structure of the porphyrin core. Contrasting magnetic behaviour of [Fe(tpp$^{\bullet}$)Cl]$^+$ (H_2tpp = 5,10,15,20-tetraphenylporphyrin) (strongly antiferromagnetic, $-2J \geqslant 500$ cm^{-1}) and [Fe(tpp$^{\bullet}$)($OClO_3$)$_2$] (ferromagnetic, $2J \approx +80$ cm^{-1}) have been explained in terms of presence of a ruffled porphyrin core in the former and a flat porphyrin core in the latter.[5–10]

Additional examples of iron porphyrins which have non-planar porphyrin cores are needed further to substantiate the structure-spin coupling mechanism correlations observed for metalloporphyrins.[5,6] We have recently characterised a variety of non-planar porphyrins and metalloporphyrins.[11] The non-planarity in these is due to the presence of short bridging chains above and below the porphyrin plane. Oxidation of the porphyrin ring is expected to enhance the non-planarity of the porphyrin ring thereby altering the magnetic properties. In view of this, we have examined the π-cation radicals of a series of deformed iron porphyrins (Fig. 1) by magnetic susceptibility measurements, ^{1}H NMR and optical spectroscopy. Furthermore, molecular mechanics simulations using MOBY[12] have been performed to establish the non-planarity of the porphyrin core in the free bases while ^{1}H NMR and optical spectral studies on iron derivatives unambiguously reveal the retention of a non-planar core in solution. An antiferromagnetic interaction has been observed between the unpaired electrons of the iron centre and the oxidised porphyrin ring both in solid and solution phases in the temperature range 80–300 K.

Results

Reaction of tris(*p*-bromophenyl)ammonium hexachloroantimonate with complexes [Fe(L^n)Cl] **1–4** (n = 1–4) in CH_2Cl_2 generates crystalline radical species [Fe(L$^{n\bullet}$)Cl][$SbCl_6$] **5–8**. Fig. 2 shows a comparison of optical spectra of **3** and its radical cation while the data for the remainder are given in Table 1. These data reveal the following: (*a*) the absorption maxima of neutral iron porphyrins are red shifted relative to the parent [Fe(tpp)Cl][13] and (*b*) upon oxidation, the Soret band shifts to lower wavelength (8–10 nm) with reduction in intensity and broadening while only small perturbations are observed for the Q bands. The IR spectra of all the oxidized species in KBr pellets show a diagnostic band in the region 1280–1290 cm^{-1} characteristic of oxidation of the porphyrin ring.[14] Cyclic voltammetry shows the first ring oxidation at 1.02, 1.04 and 1.05 V for **3**, **2** and **1** respectively, with peak separation $\Delta(E_p - E_a)$ of *ca.* 100 mV. These results can be compared with $E_{\frac{1}{2}}$ values of 1.10 ± 0.01 V observed for a series of [Fe(tpp)X] compounds for the ring oxidation.[13,15] The slightly easier oxidations relative to [Fe(tpp)X] are consistent with the presence of deformation.[16]

The pyrrole region of the ^{1}H NMR spectra of **1–4** in $CDCl_3$, recorded on a 400 MHz spectrometer is displayed in Fig. 3. The complex [Fe(tpp)Cl] shows only one peak in this region at δ 79.4. The multiplet structures observed here (except for **2**, which shows a doublet) are due to the inequivalence of the pyrrole protons thus revealing the presence of deformation in solution. The large downfield shift of the pyrrole protons is associated with predominant σ-spin delocalisation in the $d_{x^2-y^2}$ orbital.[17]

† *Supplementary data available* (No. SUP 56977, 14 pp.) atomic coordinates and selected bond lengths and angles calculated for H_2L^1 and H_2L^2 by molecular mechanics calculations. See Instructions for Authors, *J. Chem. Soc., Dalton Trans.*, 1994, Issue 1, pp. xxiii–xxviii.
Non-SI units employed: emu = $10^6/4\pi$ SI, $\mu_B \approx 9.274 \times 10^{-24}$ J T^{-1}.

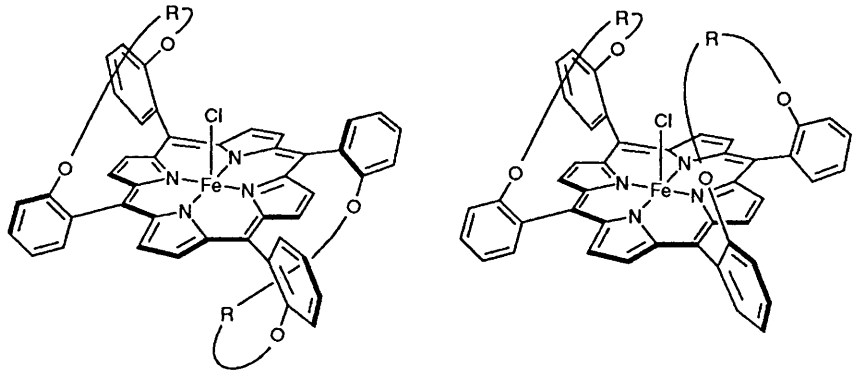

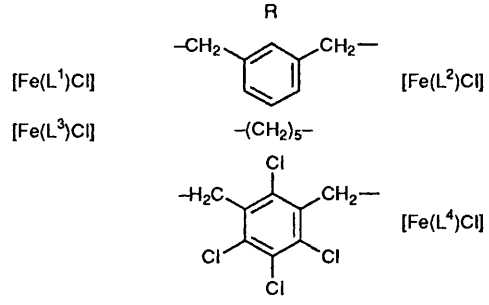

Fig. 1 Structures of various deformed iron(III) porphyrins

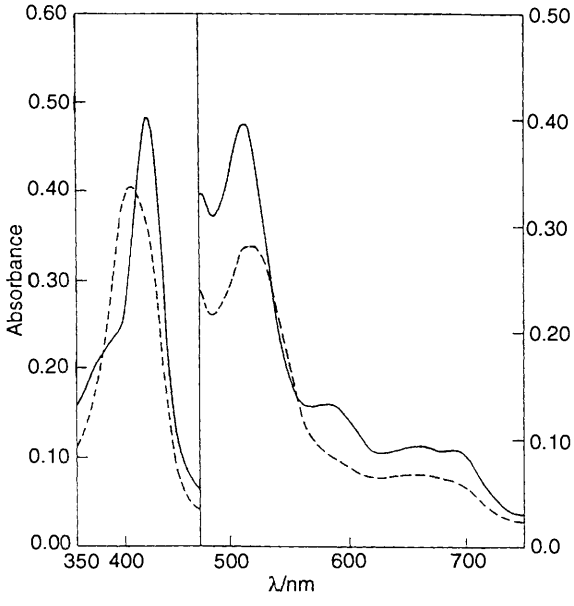

Fig. 2 Comparison of the optical absorption spectra of **3** (——) and its radical cation **7** (– – – –) in CH_2Cl_2. Concentrations used were $\approx 2 \times 10^{-5}$ mol dm^{-3} for Q-band and $\approx 2 \times 10^{-6}$ mol dm^{-3} for Soret band regions

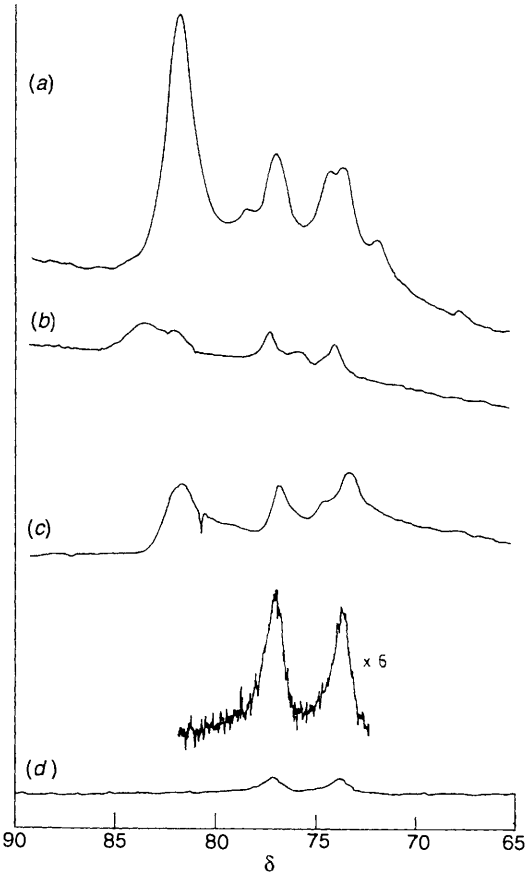

Fig. 3 Proton NMR spectra in the pyrrole proton region for (*a*) **1** (*b*) **4** (*c*) **3** and (*d*) **2** in $CDCl_3$ at 300 K

Magnetic moment measurements of the oxidised species were done both on solids and CD_2Cl_2 solutions. Fig. 4 shows the Curie–Weiss and magnetic moment plot *versus* temperature for $[Fe(L^{1\bullet})Cl][SbCl_6]$ **5** in the accessible temperature range 300–80 K and the data are listed in Table 2. The solid line of Fig. 4 represents a linear least-squares fit. The measured magnetic moments are in the range 4.8–5.1 μ_B for the various oxidised iron porphyrins **5**–**8** at 300 K both in the solid state and as CD_2Cl_2 solutions. Theoretically calculated magnetic moments for high-spin iron(III) ($S = \frac{5}{2}$) and porphyrin radical ($S = \frac{1}{2}$) are 6.9, 4.9 and 6.1 μ_B for ferromagnetically coupled, antiferromagnetically coupled and non-interacting spins respectively.[6] The measured magnetic moments imply an antiferromagnetic coupling between the metal and porphyrin-ring electrons to give an overall $S = 2$ state for all the iron porphyrin radical cations **5**–**8**.

Table 1 Electronic spectral data of various deformed iron(III) porphyrins and their cation radicals in CH_2Cl_2

Porphyrin	Soret band λ_{max}/nm (10^{-4} ε/dm^3 mol^{-1} cm^{-1}) B (0,0)	Q-bands λ_{max}/nm (10^{-3} ε/dm^3 mol^{-1} cm^{-1}) I	II[a]	III[a]	IV[a]
[Fe(tpp)Cl][b]	417 (110)	511 (13.4)	577 (13.3)	658 (2.8)	690 (3.2)
[Fe(tpp•)Cl][SbCl$_6$][b]	387	533	615	—	750
[Fe(L^1)Cl] **1**	420 (58.9)	513 (7.24)	583 (2.02)	656 (1.51)	701 (1.32)
[Fe(L$^{1•}$)Cl][SbCl$_6$] **5**	408 (36.9)	520 (4.83)	586 (1.68)	658 (1.09)	698 (0.82)
[Fe(L^2)Cl] **2**	423 (54.3)	511 (8.34)	589 (2.50)	657 (1.68)	698 (1.57)
[Fe(L$^{2•}$)Cl][SbCl$_6$] **6**	412 (38.3)	521 (4.99)	590 (1.49)	661 (1.19)	694 (0.95)
[Fe(L^3)Cl] **3**	420 (70.5)	512 (11.03)	586 (3.39)	656 (2.30)	698 (2.36)
[Fe(L$^{3•}$)Cl][SbCl$_6$] **7**	414 (43.8)	515 (11.02)	—	—	703 (2.19)
[Fe(L^4)Cl] **4**	420	511	589	656	697
[Fe(L$^{4•}$)Cl][SbCl$_6$] **8**	412	515	589	—	702

[a] Shoulder peaks. [b] From refs. 7 and 13.

Table 2 Magnetic moment data for various iron(III) deformed porphyrin cation radicals

Compound	$\mu_{eff}^{300\ K}/\mu_B$ (CD_2Cl_2)	$\mu_{eff}^{80\ K}/\mu_B$ (Solid)	$\mu_{eff}^{300\ K}/\mu_B$ (Solid)	θ/K
[Fe(tpp•)Cl][SbCl$_6$]*	6.1	—	4.8	−7.5
5	4.8	4.84	5.1	−18.9
6	4.9	4.78	4.9	−19.8
7	4.9	4.82	5.1	−19.6
8	5.0	4.80	5.1	−20.2

* From ref. 8.

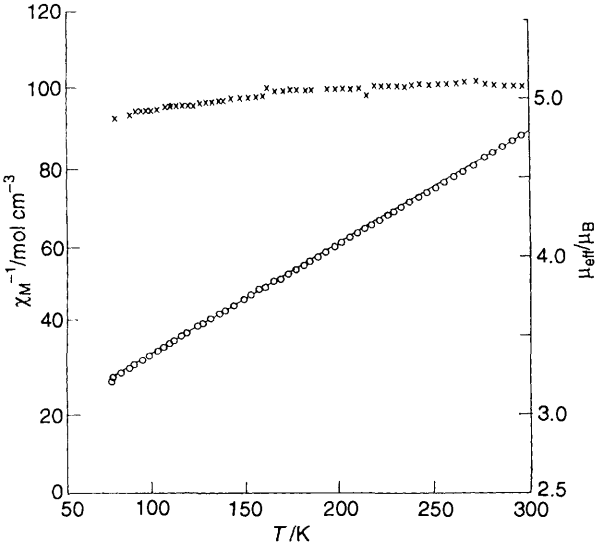

Fig. 4 Curie plot (○) of the reciprocal molar susceptibility and μ_{eff} (×) *vs.* temperature for [Fe(L$^{1•}$)Cl][SbCl$_6$] **5**

Two views of the structures for the two free-base isomers H_2L^1 and H_2L^2 calculated using the MOBY geometry optimisation program are shown in Fig. 5 with generated atomic coordinates and bond lengths and angles given in SUP 56977. The computation of energy according to the classical force field is based on the AMBER force field.[12] The force-field calculations are performed only on the fragment (and not root) centres and are limited to a maximum of 150 centres. However, for each of these centres the complete interactions to all existing centres (fragment and root) are computed exactly, so that the calculated energy value gives the energy of the fragment centre in the field of all centres.

The geometry optimisation technique utilises energy gradients based on the cartesian coordinates of the centre in order to minimise the potential energy of the system. The optimisation is divided into two operations: first the gradient is calculated at the geometry in order to fix a direction in $3n$ dimensional space, in which the potential energy minimum is determined (line search). Secondly, the resulting geometry is used as the starting geometry for the next minimisation step. These two steps (optimisation cycle) are repeated until one of the completion conditions is satisfied.

Discussion

The calculated structures shown clearly reveal the enforced deformation of the porphyrin core due to the covalent attachment of short bridging groups. The porphyrin core in the adjacent-*cis* isomer (Fig. 1) can be compared to the 'saddle conformation' described by Scheidt and Lee[18] in which the perpendicular displacements of pyrrole rings with respect to mean plane of the core are in the same direction. The distortion of the adjacent-*trans* isomer leads to a 'ruffled conformation' where the pyrrole rings are displaced alternately above and below the mean plane of the core. No major changes in these conformations are expected upon introduction of Fe^{3+} into the porphyrin core. The optical absorption red shifts of both the Soret (171–340 cm^{-1}) and Q bands (76–354 cm^{-1}) of **1**–**4** relative to [Fe(tpp)Cl] (Table 1) and the splitting of the pyrrole protons, which occur as a singlet in [Fe(tpp)Cl], into a multiplet structure justify such a conclusion.

The blue shift, broadening and intensity decrease of the Soret band and broadening of the Q bands in the electronic spectra combined with the observation of a diagnostic band around 1285 cm^{-1} in the IR spectra and the similarity of first ring oxidation potential with that of [Fe(tpp)X] derivatives suggest oxidation of the porphyrin ring in species **5**–**8** rather than of the metal centre. This implies a high-spin Fe^{III} centre with $S = \frac{5}{2}$ and a porphyrin radical with $S = \frac{1}{2}$ for the oxidised iron porphyrins **5**–**8**.

From an elegant study on the π-cation radicals of [Fe(tpp)Cl] and [Fe(tpp)(OClO$_3$)$_2$] Reed and co-workers[5–8] have related their contrasting magnetic behaviour to the structure of the porphyrin core. Crystal structures of [Fe(tpp•)Cl]$^+$ and [Fe(tpp•)(OClO$_3$)$_2$] reveal that the former has a ruffled core while the latter has a planar or flat core with effective D_{4h} symmetry at the iron centre. Because the magnetic orbitals[19] on the metal [$d_{x^2-y^2}(b_{1g})$, $d_{z^2}(a_{1g})$, $d_{xz}(e_g)$, $d_{yz}(e_g)$ and $d_{xy}(b_{2g})$] and the half-filled porphyrin ring (a_{2u}) have different symmetries, strict orthogonality is maintained between these orbitals leading to the alignment of all the spins in a parallel fashion resulting in a lowest energy $S = 3$ state. How-

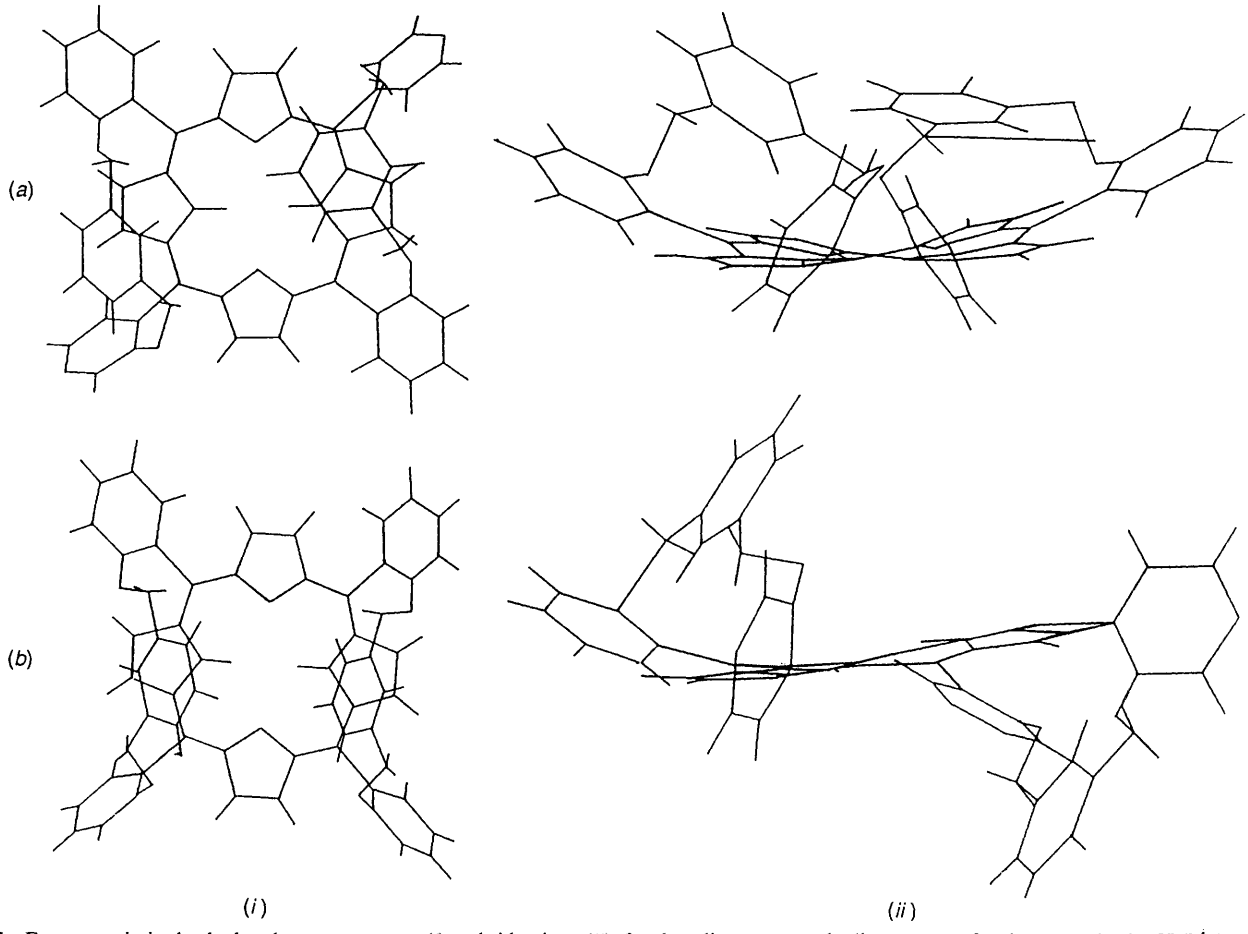

Fig. 5 Energy optimised calculated structures, top- (*i*) and side-views (*ii*), for the adjacent-*cis* and adjacent-*trans* free base porphyrins H_2L^1 (*a*) and H_2L^2 (*b*)

ever, if the core is ruffled, the D_{4h} symmetry at the iron centre is lowered probably to C_{2v} reducing the symmetry of the iron d orbitals to a_1, a_1, b_1, b_2 and a_2 and the half-filled porphyrin a_{2u} orbital to a_1. Thus, an overlap of the metal a_1 orbital and the porphyrin a_1 orbital results in pairing of the electrons suggesting an $S = 2$ ground state.[5] From this, they concluded that the presence of a planar or flat core leads to a ferromagnetic coupling while that of a ruffled core results in an antiferromagnetic coupling. The measured magnetic moments for the two radical species are in excellent agreement with this conclusion.

The magnetic moments measured for the radical species generated in the present study both in the solid state and as CD_2Cl_2 solutions suggest an antiferromagnetic coupling between the iron and the unpaired porphyrin electrons. Apparently, the presence of a deformed core in the iron porphyrins described here destroys the orthogonality between the d orbitals of iron and the half-filled porphyrin a_{2u} orbital allowing an intramolecular d–π coupling necessary for the antiferromagnetic exchange. It is pertinent that Goff and co-workers[9,10] on the basis of NMR and magnetic moment measurements concluded that oxidised five-co-ordinate [Fe^{III}-(tpp$^{\bullet}$)X] complexes with weak axial ligands such as ClO_4^- or $SO_3CF_3^-$ retained the spin admixed $S = \frac{5}{2}, \frac{3}{2}$ configuration in solution. However, the similar magnitude of magnetic moment values for the present oxidised complexes **5**–**8** both as solids and as CD_2Cl_2 solutions, and their larger values of Curie-Wiess constants θ (measured by extrapolation of the plot shown in Fig. 4) relative to that of [Fe(tpp$^{\bullet}$)Cl]$^+$ [8] leads us to rule out the possibility of an admixed spin configuration for the radical cations discussed here.

Further evidence for antiferromagnetic coupling in **5**–**8** comes from preliminary ^{1}H NMR studies on **1** and its cation radical in $CDCl_3$. The ^{1}H NMR spectrum of **1** shows resonances at δ 78.5 (m, 8 H, β-pyrrole), 15.3, 12.7 (m, 8 H, *m*-H), 6.67 (m, 4 H, *o*-H), 4.67 (m, 4 H, *p*-H) and a broad multiplet at δ −4.5 (10 H, bridging $-CH_2-$, $w_{\frac{1}{2}}$ = 499 Hz) while its radical cation under the same conditions shows resonances at δ 69 (m, 8 H, β-py), 46 (m, 4 H, *o*-H), 26.2 (m, 4 H, *p*-H), −14 (m, 8 H, *m*-H) and −3.66 (10 H, bridging $-CH_2-$, $w_{\frac{1}{2}}$ = 533 Hz). Thus the direction and magnitude of shifts of the pyrrole, *ortho*-, *meta*- and *para*-phenyl protons in [Fe($L^{1\bullet}$)Cl][$SbCl_6$] **5** relative to **1** is consistent with antiferromagnetic coupling for the five-co-ordinate, high-spin iron(III) porphyrin cation radicals.[5,9]

In summary, the present study has substantiated the emerging generality between the structure of the macrocycle and the metal–ligand magnetic interactions in high-spin iron(III) porphyrin radical-cation complexes that ruffled cores lead to antiferromagnetic coupling while planar or flat cores result in a ferromagnetic coupling, as proposed by Reed and co-workers.[5–8] However, this study also reveals that the presence of ruffled cores need not necessarily lead to dimerisation of the porphyrin, a suggestion made by Reed and co-workers[20] based on X-ray structures of many metal–tetraphenylporphyrin radical cations.

Experimental

(*a*) *Syntheses*.—The synthesis of free-base porphyrins has been described earlier.[11a,c] The oxidant tris(*p*-bromophenyl)-ammonium hexachloroantimonate was procured from E. Merck (Germany).

[Fe(L^1)Cl] **1**. A solution of an excess of freshly prepared anhydrous iron(II) chloride and a deficit of the freebase

porphyrin (0.100 g, 0.0001 mmol) in dry dimethylformamide (10 cm^3) was heated under reflux for 6 h in an argon atmosphere. The progress of the reaction was monitored by electronic absorption spectroscopy. Upon completion the solution was filtered and evaporated to dryness *in vacuo* and the resultant solid was extracted with chloroform (100 cm^3). The organic layer was washed with dilute $NaHCO_3$ (3 × 100 cm^3) and evaporated to dryness. The crude iron(III) porphyrin was chromatographed over silica gel (60–120 mesh) using chloroform as eluent. The fast moving band was collected. The solution was evaporated and the resultant solid was dried under high vacuum (0.060 g, 45%). The compound was recrystallised from chloroform–methanol.

FAB mass spectrum: *m/z* 974 (calc. 974) (Found: C, 72.95; H, 3.90; N, 5.70. $C_{60}H_{40}ClFeN_4O_4$ requires C, 73.90; H, 4.10; N, 5.75%). The other iron derivatives **2–4** were synthesised as above.

[Fe(L^2)Cl]. FAB mass spectrum: *m/z* 974 (calc. 974) (Found: C, 73.90; H, 4.20; N, 5.80. $C_{60}H_{40}ClFeN_4O_4$ requires C, 73.90; H, 4.10; N, 5.75%).

[Fe(L^3)Cl] **3**. FAB mass spectrum: *m/z* 904 (calc. 904) (Found: C, 71.50; H, 4.80; N, 6.25. $C_{54}H_{44}ClFeN_4O_4$ requires C, 71.70; H, 4.90; N, 6.20%).

[Fe(L^4)Cl] **4**. FAB mass spectrum: *m/z* 1248 (calc. 1248) (Found: C, 57.95; H, 2.65; N, 4.55. $C_{60}H_{32}Cl_9FeN_4O_4$ requires C, 57.75; H, 2.60; N, 4.50%).

[Fe($L^{1\bullet}$)Cl][$SbCl_6$] **5**. A dichloromethane solution of **1** (0.010 g, 0.0102 mmol) was stirred under argon for 5 min. Then 1.1 equivalents of tris(*p*-bromophenyl)ammonium hexachloroantimonate (0.0092 g, 0.0113 mmol) dissolved separately in dry CH_2Cl_2 was added slowly to the porphyrin solution. The light greenish colour observed during the initial stages of the addition disappeared upon progress of the reaction. Stirring was continued under argon for a further 3 h. Completion of the reaction was monitored by absorption spectroscopy. The reaction mixture was filtered and the solution concentrated to the minimum volume under vacuum and the product was precipitated with hexane. The compound was filtered off, washed several times with hexane and recrystallised from chloroform–hexane. The dark black crystals were dried and stored in vacuum (0.006 g, 45%) (Found: C, 54.25; H, 3.10; N, 4.35. $C_{60}H_{40}Cl_7FeN_4O_4Sb$ requires C, 55.00; H, 3.10; N, 4.25%).

Similar procedures were used for the synthesis of other oxidised derivatives **6–8**.

[Fe($L^{2\bullet}$)Cl][$SbCl_6$] **6** (Found: C, 55.05; H, 3.00; N, 4.20. $C_{60}H_{40}Cl_7FeN_4O_4Sb$ requires C, 55.00; H, 3.10; N, 4.25%).

[Fe($L^{3\bullet}$)Cl][$SbCl_6$] **7** (Found: C, 52.25; H, 3.40; N, 4.40. $C_{54}H_{44}Cl_7FeN_4O_4Sb$ requires C, 52.35; H, 3.60; N, 4.50%).

[Fe($L^{4\bullet}$)Cl][$SbCl_6$] **8** (Found: C, 45.60; H, 2.15; N, 3.65. $C_{60}H_{32}Cl_{15}FeN_4O_4Sb$ requires C, 45.55; H, 2.05; N, 3.55%).

(*b*) *Measurements*.—The UV/VIS and IR spectrometers employed and details of the cyclic voltammetry measurements in the present study are described in our earlier work.[11] Proton NMR spectra were recorded on a Bruker 400 MHz spectrometer and C, H, N analysis was done on a Heraeus Carlo Erba 1108 elemental analyser. Variable-temperature magnetic susceptibilities on powders were measured between 80 and 300 K on a computer controlled Faraday Magnetometer (models 300 and 321), George Associates, Berkeley, CA. A data translation A/D board and AT computer were used to monitor the microbalance output and temperature readings. The instrument was calibrated with $Hg[Co(NCS)_4]$ and had an absolute accuracy of 0.5%. The raw data were corrected for the susceptibility of the holder and diamagnetism of the ligands (8.72×10^{-6} emu units). Molecular mechanics calculations were carried out using MOBY (molecular modelling on the PC) software version 1.4 (copyright Springer, Berlin, 1991). The components of the energy terms in the calculations are described in detail elsewhere.[12]

Acknowledgements

T. K. C. thanks the Department of Science and Technology, Government of India, New Delhi for financial support of this work. Thanks are also due to Professor S. Mitra, Tata Institute for Fundamental Research, Bombay and Dr. R. Roy, Central Drug Research Institute, Lucknow for help in variable-temperature magnetic susceptibility and NMR measurements respectively.

References

1 C. E. Schultz, P. W. Devaney, H. Winkler, P. G. Debrunner, N. Doan, R. Chiang, R. Rutter and L. P. Hager, *FEBS Lett.*, 1979, **103**, 102.
2 J. E. Roberts, B. M. Hoffman, R. Rutter and L. P. Hager, *J. Biol. Chem.*, 1981, **256**, 2118.
3 C. E. Schulz, R. Rutter, J. T. Sage, P. G. Debrunner and L. P. Hager, *Biochemistry*, 1984, **23**, 4743; D. Mandon, R. Weiss, K. Jayaraj, A. Gold, J. Terner, E. Bill and A. K. Trautwein, *Inorg. Chem.*, 1992, **31**, 4404.
4 R. Rutter, L. P. Hager, H. Dhonau, M. Hendrich, M. Valentine and P. G. Debrunner, *Biochemistry*, 1984, **23**, 6809.
5 P. Gans, G. Buisson, E. Duee, J. C. Marchon, B. S. Erler, W. F. Scholz and C. A. Reed, *J. Am. Chem. Soc.*, 1986, **108**, 1223.
6 B. S. Erler, W. F. Scholz, Y. J. Lee, W. R. Scheidt and C. A. Reed, *J. Am. Chem. Soc.*, 1987, **109**, 2644.
7 W. F. Scholz, C. A. Reed, Y. J. Lee, W. R. Scheidt and G. Lang, *J. Am. Chem. Soc.*, 1982, **104**, 6791.
8 G. Buisson, A. Deronzier, E. Duee, P. Gans, J. C. Marchon and J. R. Regnard, *J. Am. Chem. Soc.*, 1982, **104**, 6793.
9 A. D. Boersma and H. M. Goff, *Inorg. Chem.*, 1984, **23**, 1671.
10 H. M. Goff and M. A. Phillippi, *J. Am. Chem. Soc.*, 1983, **105**, 7567.
11 (*a*) D. Reddy and T. K. Chandrashekar, *J. Chem. Soc., Dalton Trans.*, 1992, 619 (*b*); D. Reddy, T. K. Chandrashekar and H. Vanwilligen, *Chem. Phys. Lett.*, 1993, **202**, 120; (*c*) M. Ravikanth, D. Reddy, A. Misra and T. K. Chandrashekar, *J. Chem. Soc., Dalton Trans.*, 1993, 1137; (*d*) M. Ravikanth, D. Reddy and T. K. Chandrashekar, *J. Photochem. Photobiol. A: Chem.*, 1993, **72**, 61; (*e*) M. Ravikanth and T. K. Chandrashekar, *J. Photochem. Photobiol. A: Chem.*, 1993, **74**, 181.
12 S. J. Weiner, P. A. Kollman, D. A. Case, U. C. Singh, C. Ghio, G. Alagona, S. Profeta, jun. and P. Weiner, *J. Am. Chem. Soc.*, 1984, **106**, 765.
13 M. A. Phillippi and H. M. Goff, *J. Am. Chem. Soc.*, 1982, **104**, 6026.
14 E. T. Shimomura, M. A. Phillippi, H. M. Goff, W. F. Scholz and C. A. Reed, *J. Am. Chem. Soc.*, 1981, **103**, 6778.
15 M. A. Phillippi, E. T. Shimomura and H. M. Goff, *Inorg. Chem.*, 1981, **20**, 1322.
16 J. Y. Becker, D. Dolphin, J. B. Paine and T. Wijesekera, *J. Electroanal. Chem., Interfacial Electrochem.*, 1984, **164**, 335.
17 G. N. Lamar and F. A. Walker, *The Porphyrins*, ed. D. Dolphin, Academic Press, New York, 1979, vol. 4, p. 198.
18 W. R. Scheidt and Y. J. Lee, *Struct. Bonding (Berlin)*, 1987, **64**, 1.
19 O. Khan, *Inorg. Chim. Acta*, 1982, **62**, 3.
20 H. Song, C. A. Reed and W. R. Scheidt, *J. Am. Chem. Soc.*, 1989, **111**, 6867; K. M. Barkigia, L. D. Spaulding and J. Fajer, *Inorg. Chem.*, 1983, **22**, 349; H. Song, C. A. Reed and W. R. Scheidt, *J. Am. Chem. Soc.*, 1989, **111**, 6865.

Received 23rd *June* 1993; *Paper* 3/03615D